

Performance Analysis of OFDM with Peak Cancellation Under EVM and ACLR Restrictions

Tomoya Kageyama *Student member, IEEE*, Osamu Muta, *Member, IEEE*,
and Haris Gacanin, *Senior Member, IEEE*

Abstract—This paper presents performance analysis of an adaptive peak cancellation method to reduce the high peak-to-average power ratio (PAPR) for OFDM systems, while keeping the out-of-band (OoB) power leakage as well as an in-band distortion power below the pre-determined level. In this work, the increase of adjacent leakage power ratio (ACLR) and error vector magnitude (EVM) are estimated recursively using the detected peak amplitude. We present analytical framework for OFDM-based systems with theoretical bit error rate (BER) representations and detection of optimum peak threshold based on predefined EVM and ACLR requirements. Moreover, the optimum peak detection threshold is selected based on the optimal design to maintain the predefined distortion level. Thus, their degradations are automatically restricted below the pre-defined levels which correspond to target OoB radiation. We also discuss the practical design of peak-cancellation (PC) signal with target OoB radiation and in-band distortion through optimizing the windowing size of the PC signal. Numerical results show the improvements with respect to both achievable bit error rate (BER) and PAPR with the PC method in eigen-beam space division multiplexing (E-SDM) systems under restriction of OoB power radiation. It can also be seen that the theoretical BER shows good agreements with simulation results.

Index Terms—PAPR, ACLR, EVM, OoB radiation, OFDM.

I. INTRODUCTION

FUTURE wireless communication systems require robust communication over a frequency-selective fading channel [1], such as orthogonal frequency division multiplexing (OFDM) with multi-input multi-output (MIMO) technologies. One of the technical issues in MIMO-OFDM is the reduction of peak-to-average power ratio (PAPR).

Existing PAPR reduction techniques can be categorized into probabilistic-based approach [3]-[13], coding-based [14]-[16], and limiter (deliberate clipping) [17]-[32]. Contemporary communication systems rely on a simple PAPR reduction technique without any additional processing at the receiver end. Deliberate clipping and filtering (C&F)[17]-[20][28]-[31] is an attractive technique from the viewpoint of its simple implementation, but it introduces nonlinear degradations. In C&F, filtering is used to remove OoB radiation, but it causes the re-growth of signal amplitude after filtering. Other related approaches such as peak windowing, peak cancellation, and

companding (e.g.,[21]-[27][32]) have also been investigated. In principle, C&F and its simplified versions produce nonlinear distortion that may be measured by using error vector magnitude (EVM) and adjacent channel leakage power ratio (ACLR). To cope with them, initial studies of peak cancellation under out-of-band radiation has been presented in [26],[27]. However, in these works, the peak detection threshold level is empirically determined and also the optimum peak detection threshold and bit error rate (BER) analysis are not theoretically given. From the practical system design point of view, they should be kept below a pre-defined optimum threshold. An analytical evaluation of their impacts on transmission system design is an important study item. This is even more important since the bit error rate (BER) performance of the pre-coded OFDM system is highly sensitive to nonlinear degradations.

Main contributions are as follows.

- Firstly, we present a performance analysis of an adaptive peak cancellation method to keep EVM and ACLR below permissible level for multi-input multi-output (MIMO)-OFDM system. In this method, an amplitude that exceeds a given threshold is suppressed repeatedly by efficient design of peak cancellation (PC) signal, while optimizing the system performance for pre-defined ACLR and EVM. We present an efficient distortion estimation method for linearly precoded MIMO-OFDM, where the increases of ACLR and EVM are estimated recursively using the detected peak amplitude, respectively. We confirm that their degradations are restricted below the pre-defined levels which correspond to OoB radiation and the level of degradation per subcarrier.
- Secondly, differently from a primitive version of our proposed method in [27]*, this paper presents an analytical framework for OFDM-based systems with theoretical BER representations and detection of optimum peak threshold (i.e., theoretically achieved PAPR lower bound) based on EVM and ACLR. In this framework, the optimum peak detection threshold is selected based on a theoretical design to achieve the predefined distortion level. In other words, achieved PAPR lower bound at pre-defined ACLR and EVM is theoretically given as the optimum threshold level.
- In addition, we present theoretical BER representations of OFDM with the peak cancellation under EVM and ACLR restrictions for single antenna and multi-antenna systems, respectively. We clarify that signal distortion due to the

T. Kageyama is with Graduate School of Information Science and Electrical Engineering, Kyushu University in Japan. O. Muta is with Center for Japan-Egypt Cooperation in Science and Technology, Kyushu University in Japan (e-mail: muta@ait.kyushu-u.ac.jp, muta@ieee.org). H. Gacanin is with Customer Experience Division of Alcatel-Lucent in Belgium.

*This work was presented in part at the 2015 IEEE International Symposium on Personal Indoor and Mobile Radio Communications (IEEE PIMRC 2015) [27].

peak cancellation is approximated with a random variable which follows Gaussian distribution whose variance and average power is determined based on the optimum peak detection threshold. We confirm that achievable PAPR is minimized using the proposed framework comparable to those in repeated C&F method, while restricting the distortions within pre-defined levels.

- We also discuss the practical design of peak-cancellation signal, where achievable OoB radiation and in-band distortion can be adjusted by optimizing the windowing size of the PC signal. We evaluate and discuss the advantage of our designed method in terms of BER, complementary cumulative distribution function (CCDF) of PAPR as well as computational complexity for precoded MIMO-OFDM systems under the restriction of OoB power radiation. Numerical results clarify the effectiveness of our proposed peak cancellation.

II. RELATED WORKS

Limiter based PAPR reduction techniques have been investigated for OFDM systems in the literature. In particular, various C&F based approaches are presented such as in [20][28]-[32]. In [20], an adaptive selection method of peak detection threshold is proposed to achieve fast convergence in repeated C&F. This method is effective in reducing the required number of iterations in C&F. However, in-band distortion due to clipping is not restricted below a pre-defined level. In [28], an optimized filtering method is proposed for repeated C&F in which filter characteristic is optimized to minimize in-band distortion (i.e., EVM) under PAPR constraint while limiting the OoB radiation. Using this method, the required number of repetitions is reduced compared with traditional repeated C&F. In [29], a modified repeated C&F method is presented where the clipped signal is optimized by minimizing the increase of in-band distortion at each clipping iteration under PAPR constraint. This method is also effective in reducing the required number of iterations in repeated C&F. However, the above methods still require repeated filtering operations to limit OoB radiation which results in increased computational complexity. In [30], a simplified C&F technique using a neural network is proposed. In this method, band-limited clipped signal is approximately generated with a learning-based approach without actual filtering process. Thus, the required complexity to reduce PAPR is reduced. However, the bit error rate is degraded due to inaccurate approximation as modulation order increases. Thus, more complicated learning method may be needed for signals with higher-order modulation. In [31], a repeated C&F method that adaptively determines the clipping threshold is proposed. Although this method does not require a pre-defined threshold, in-band distortion is not restricted below a pre-defined level. In [32], a new limiter based companding function was proposed to suppress peak amplitude effectively. However, companding transformation causes OoB radiation due to nonlinearity of companding function.

Unlike the above approaches, in this paper, we designed an effective peak cancellation method that automatically restricts EVM and ACLR below the optimum predefined level, while

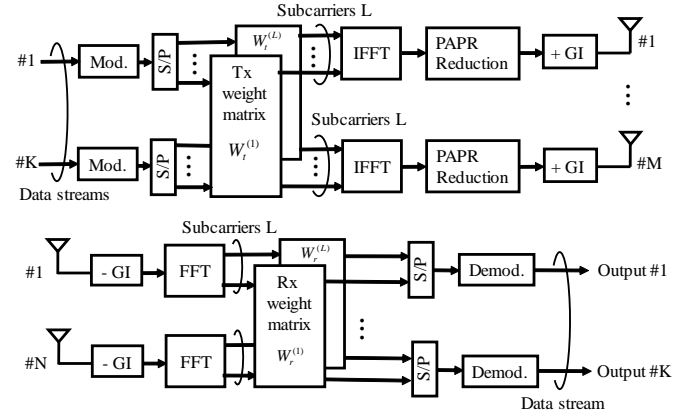


Fig. 1. System block diagram.

reducing the peak amplitude below the threshold level with lower complexity than the conventional repeated C&F.

III. MATHEMATICAL SIGNAL REPRESENTATION

A. System Model

Figure 1 illustrates an E-SDM OFDM system model, where M , N , and K denote the number of transmit antennas, receive antennas, and data streams, respectively. \mathbf{W}_t^l and \mathbf{W}_r^l denote precoding and post-coding matrices on the l -th subcarrier, respectively, where $l = 1, \dots, L$, and L denotes the number of subcarriers. Here, the transmit data vector of the l -th subcarrier $\mathbf{x}^l = [x_1^l, \dots, x_k^l, \dots, x_K^l]^T$ is multiplexed by the precoding matrix $\mathbf{W}_t^l = [\mathbf{w}_{t1}^l, \dots, \mathbf{w}_{tk}^l, \dots, \mathbf{w}_{tK}^l]$, where $\mathbf{w}_{tk}^l = [w_{tk1}^l, \dots, w_{tkm}^l, \dots, w_{tkM}^l]^T$ is the l -th column vector of \mathbf{W}_t^l for the k -th data stream and superscript T stands for transposed matrix. In E-SDM, left singular vector and right singular vector of the channel matrix are used as precoding and post-coding matrices, respectively. \mathbf{H}^l stands for $N \times M$ matrix of the l -th subcarrier defined as

$$\mathbf{H}^l = \begin{pmatrix} h_{11}^l & \dots & h_{1M}^l \\ \vdots & h_{nm}^l & \vdots \\ h_{N1}^l & \dots & h_{NM}^l \end{pmatrix}, \quad (1)$$

where h_{nm} denotes impulse response of the path. Here, the m and n denote the transmit antenna index and the receive antenna index, respectively. Using with singular value decomposition (SVD), \mathbf{H}^l can be decomposed into

$$\mathbf{H}^l = \mathbf{U}_l \Sigma_l \mathbf{V}_l^H, \quad (2)$$

where \mathbf{U}_l and \mathbf{V}_l^H are left and right singular vector of \mathbf{H}^l , and $(\cdot)^H$ means complex conjugate operation. $\Sigma_l = \text{diag}(\sqrt{\lambda_1^l}, \sqrt{\lambda_2^l}, \dots, \sqrt{\lambda_M^l})$ is a diagonal matrix and $\sqrt{\lambda_m^l}$ is the singular value of m -th stream. Transmit and receive spatial filter are defined as $\mathbf{W}_t^l = \mathbf{V}_l$ and $\mathbf{W}_r^l = \mathbf{U}_l^H$. The precoded QAM data stream is modulated with inverse fast Fourier transform (IFFT) and then PAPR reduction technique is applied at each transmits antenna. The guard interval (GI) is added to every symbol to remove inter-symbol interference. Perfect channel estimation is assumed.

After removing GI and carrying out FFT processing, the received signal is multiplied by the post coding matrix $\mathbf{W}_r^l = [\mathbf{w}_{r1}^l, \dots, \mathbf{w}_{rk}^l, \dots, \mathbf{w}_{rK}^l]^T$, where $\mathbf{w}_{rn}^l = [w_{rn1}^l, \dots, w_{rnk}^l, \dots, w_{rnK}^l]^T$ denotes the n -th post-coding vector of the l -th subcarrier. Hence, the de-multiplexed signal vector $\mathbf{y}^l = [y_1^l, \dots, y_k^l, \dots, y_K^l]^T$ of the l -th subcarrier is given as

$$\begin{aligned} \mathbf{y}^l &= \mathbf{W}_r^l (\mathbf{H}^l \mathbf{W}_t^l \mathbf{x}^l + \mathbf{n}^l) \\ &= \mathbf{U}_l^H (\mathbf{H}^l \mathbf{V}_l \mathbf{x}^l + \mathbf{n}^l) \\ &= \mathbf{U}_l^H (\mathbf{U}_l \Sigma_l \mathbf{V}_l^H \mathbf{V}_l \mathbf{x}^l + \mathbf{n}^l) \\ &= \Sigma_l \mathbf{x}^l + \mathbf{U}_l^H \mathbf{n}^l, \end{aligned} \quad (3)$$

where \mathbf{U}_l and \mathbf{V}_l are unitary matrices and $\mathbf{n}^l = [n_1, \dots, n_n, \dots, n_N]^T$ is an additive white Gaussian noise (AWGN) vector at each receive antenna.

B. Definitions of ACLR and EVM

In this paper, we evaluate the amount of OoB radiations as ACLR which is defined as

$$\text{ACLR} = \int_{f_U, f_L} \frac{S(\omega)}{S_t} d\omega, \quad (4)$$

Here, $S_t = \frac{1}{2} E[|x_k^l|^2]$ denotes the average power of the transmit signal and $S(\omega)$ is the power spectral density of the transmitted signal. Let f_U - and f_L denote the measured ACLR at an upper and lower band, respectively. The permissible maximum ACLR is set to -50 dB for transmitting signals at every antennas.

We also evaluate in-band distortion by measuring EVM which is defined as:

$$\text{EVM} = \sum_{l=-L/2+1}^{L/2} |X_l - \tilde{X}_l|^2 / \sum_{l=-L/2+1}^{L/2} S_t[l], \quad (5)$$

where $S_t[l]$ is the average power of the l -th subcarrier signal. X_l and \tilde{X}_l denote the complex signals at the l -th subcarrier (after FFT operation) without and with PAPR reduction, respectively. In E-SDM case, X_l and \tilde{X}_l are defined as complex signals and replicated at the l -th subcarrier of each eigen-channel by Eq. (3).

IV. ADAPTIVE PEAK-CANCELLATION TECHNIQUE

Figure 2 shows the block diagram of our designed peak cancellation which consists of five steps, i.e., PC signal generation, selection of the peak detection threshold, peak detector, distortion estimation, and PC signal scaling, where $x^{(m,i)}(t)$ denotes input signal at m -th antenna at i -th repetition. The first two blocks ("PC signal generation" and "selection of the peak detection threshold") are carried out beforehand. In each transmission frame, whenever the maximum amplitude $x_{max}^{(m,i)}$ exceeding the threshold A_{th} is detected at the peak detector, the distortion estimation is carried out using a recursive method, and it decides whether both ACLR and EVM are below their given values or not (i.e., binary decision; "Y" or "N"). An average EVM value and the maximum ACLR value over all transmit antennas are estimated, and then if the estimated values are below the pre-defined values, the

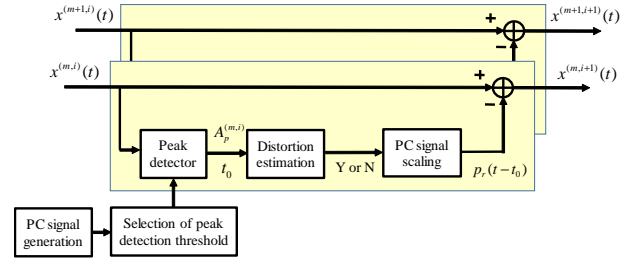


Fig. 2. Block diagram of the proposed method, where $x^{(m)}(t, i)$ denotes the transmit signal at m -th antenna after adding i -th PC signal.

amplitude of the PC signal is scaled to $A_p^{(m,i)} = x_{max}^{(m,i)} - A_{th}$. Then, the scaled PC signal is added to reduce $x_{max}^{(m,i)}$ to A_{th} . Otherwise, the peak cancellation procedure stops. The details of each step are explained below.

(Step 1) Peak Cancellation Signal Generation

Whenever the maximum signal amplitude exceeds a given threshold level A_{th} , the maximum peak is suppressed by adding a PC signal. Here, the PC signal is a scaled OFDM symbol whose subcarriers are added up to be in-phase at a given symbol time instant. The PC signal is generated by scaling the following basic function $g(t)$ as

$$g(t) = \frac{1}{L} \sum_{l=-L/2+1}^{L/2} p_l(t) e^{j\omega_l t}, \quad (6)$$

where $p_l(t)$ is the transmit pulse at the l -th subcarrier. In this paper, we assume that $p_l(t)$ is the same rectangular pulse on all subcarriers whose amplitude is unity. The time-domain waveform of $g(t)$ is truncated by a windowing function $w(t)$; the truncated version of $g(t)$ is given as

$$g'(t) = w(t)g(t). \quad (7)$$

We use the following windowing function to truncate the peak cancellation signal waveform:

$$w(t) = \begin{cases} 0 & (T_2 < |t|) \\ \frac{1}{2} + \frac{1}{2} \cos \frac{\pi(|t| - T_1)}{T_2 - T_1} & (T_1 < |t| \leq T_2) \\ 1 & (|t| \leq T_1), \end{cases} \quad (8)$$

where $0 < T_1 \leq T_2$. Here, T_1 is a design parameter to optimize distortions appeared after peak cancellation. T_2 denotes window size of $w(t)$. The truncated PC signal waveform and its frequency spectrum of $g'(t)$ are illustrated in Figs. 3 (a) and (b), respectively. Here, parameters of windowing function are given as $(T_1, T_2) = (T/8, T/4)$. The PC signal explicitly exhibits high peak amplitude which is utilized to reduce the PAPR of OFDM.

(Step 2) Selection of Peak Detection Threshold

In the proposed method, the optimum peak detection threshold should be selected so that the signal amplitude is suppressed below the threshold level, while EVM and ACLR are

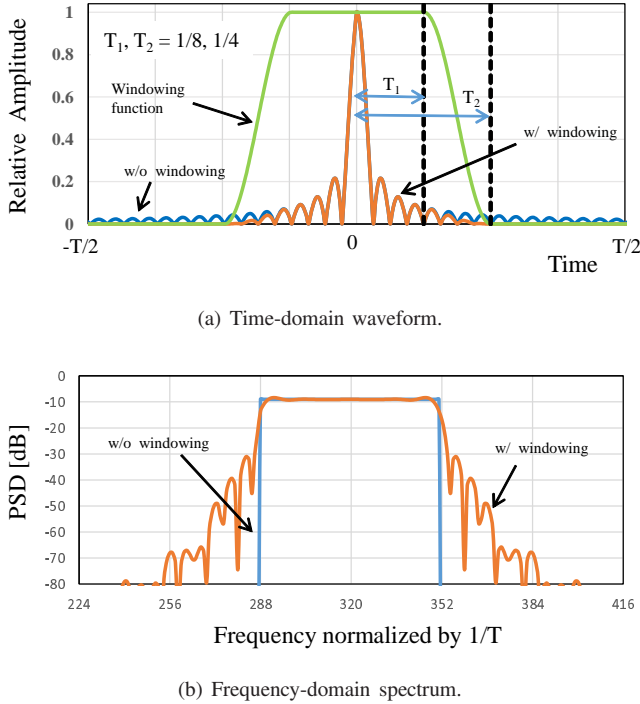


Fig. 3. An example of peak cancellation (PC) signal.

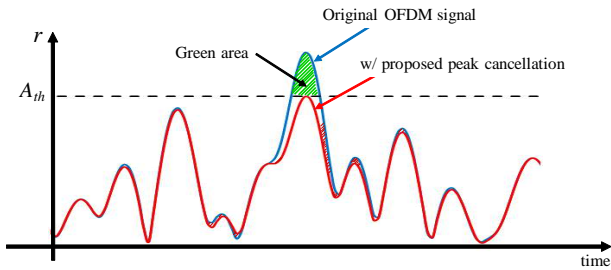


Fig. 4. Illustration of the peak cancellation effect.

kept below the pre-defined values. This subsection describes the optimum threshold selection. Figure 4 illustrates an example of an OFDM signal waveform. In this figure, red and blue lines show the signal with and without the proposed peak cancellation, respectively. The green-shaded area corresponds to signal amplitude exceeding the peak detection threshold A_{th} . As illustrated in Fig. 4, adding the PC signal distorts the OFDM signal and increases both EVM and ACLR.

Figure 5 illustrates the relation between the scaling factor of the PC signal and the peak detection threshold, where ζ and A_{th} denote the maximum amplitude of the OFDM signal and the peak detection threshold, respectively. As illustrated in Fig. 5, when the maximum amplitude ζ exceeds the threshold level A_{th} , OFDM signal amplitude is reduced to the threshold level by adding the PC signal whose amplitude is scaled to $\zeta - A_{th}$. Since the scaled PC signal is given as $(\zeta - A_{th})g'(t)$,

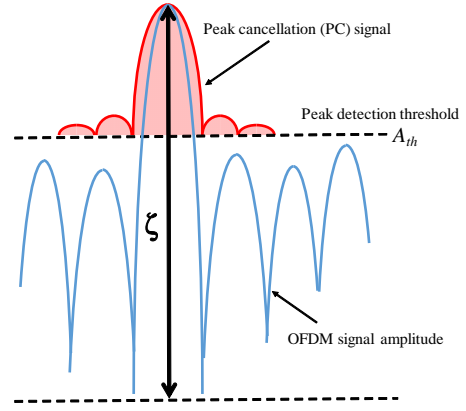


Fig. 5. Modeling of signal distortion due to PC signal addition.

the energy of the scaled PC signal is calculated as

$$\begin{aligned}
 E(\zeta - A_{th}) &= \int_{-T_2}^{T_2} (\zeta - A_{th})^2 g'^2(t) dt \\
 &= (\zeta - A_{th})^2 \int_{-\infty}^{\infty} G'^2(\omega) d\omega \\
 &= (\zeta - A_{th})^2 \left(\int_{f_{in}} G'^2(\omega) d\omega + \int_{f_{out}} G'^2(\omega) d\omega \right) \\
 &\equiv (\zeta - A_{th})^2 (E_i + E_o), \tag{9}
 \end{aligned}$$

where f_{in} and f_{out} denote bandwidths to measure EVM and ACLR, respectively. Here, $G'(t) = \int_{-\infty}^{\infty} g'(t) e^{-j\omega t} dt$. E_i and E_o denote in-band power and out-of-band power of PC signal, respectively. Statistical distribution of instantaneous power of the OFDM signal follows exponential distribution as

$$r(\zeta^2) = \frac{1}{\sigma^2} \exp\left(-\frac{\zeta^2}{\sigma^2}\right), \tag{10}$$

where ζ^2 and $S_t = \sigma^2$ denotes instantaneous power and average power of OFDM signal, respectively. Thus, the average signal distortion due to peak cancellation is calculated as

$$\begin{aligned}
 S_d &= \int_{A_{th}}^{\infty} E(\zeta - A_{th}) r(\zeta^2) d\zeta^2 \\
 &= (E_i + E_o) \int_{A_{th}}^{\infty} (\zeta - A_{th})^2 r(\zeta^2) d\zeta^2. \tag{11}
 \end{aligned}$$

The in-band distortion power is given as

$$S_{in} = E_i \int_{A_{th}}^{\infty} (\zeta - A_{th})^2 r(\zeta^2) d\zeta^2. \tag{12}$$

Assuming $E_i \gg E_o$, the normalized signal distortion is restricted as

$$\frac{S_d}{S_t} \approx \frac{S_{in}}{\sigma^2} \leq \frac{e_r}{\sigma^2}, \tag{13}$$

where the average power of the signal is $S_t = \sigma^2$ and $\frac{e_r}{\sigma^2}$ denotes the pre-determined value of the maximum acceptable EVM. Hence, the minimum (optimum) peak detection threshold A_{th}^o that meets the EVM requirement is given as

$$\int_{A_{th}^o}^{\infty} (\zeta - A_{th}^o)^2 r(\zeta^2) d\zeta = \frac{e_r}{E_i}. \tag{14}$$

Here, $(A_{th}^o)^2$ corresponds to the peak power of the OFDM signal after peak cancellation. Using Eq.(14), the optimum threshold A_{th}^o to achieve pre-determined EVM value can be theoretically obtained.

(Step 3) Peak Detection

In Fig. 2, the remaining three steps (i.e., “peak detection”, “distortion estimation”, and “PC signal scaling”) are repeated until the maximum value is below the threshold value unless ACLR or EVM exceeds their pre-defined values. At the first step, when the peak amplitude of the OFDM signal at m -th antenna exceeds the selected peak detection threshold at time instance $t = t_0$, the difference between the detected peak amplitude and the detection threshold, $A_p^{(m,i)}$, is calculated. In the next step, the increase of ACLR and EVM is estimated using the detected value $A_p^{(m,i)}$.

(Step 4) Distortion Estimation

In multi-stream transmission in MIMO-OFDM, the peak cancellation is carried out to suppress the peak amplitude below the peak detection threshold under constraints of EVM and ACLR, where EVM and ACLR requirements are defined as an average value and the maximum value over all antennas, respectively.

Since the truncated signal $g'[s] = g'(s\Delta t)$ has out-of-band spectrum, it is clear that out-of-band radiation and in-band distortion appears by adding $g'[s]$ to the transmit signal, where Δt denotes sampling interval. Here,

$$G'[l]\mathcal{F}[g'[s]] = W[l]*G[l],$$

where \mathcal{F} and $*$ denote discrete Fourier transform and convolution operator, respectively. $G[l]$ and $W[l]$ are frequency spectrum of the PC signal $g[s]$ and the window function $w[s]$, respectively.

Let Δp_o and Δp_{in} denote OoB signal power and in-band signal power of $g'(t)$. Note that Δp_o and Δp_{in} are known values (calculated beforehand). Hence, when $G'[l]$ is added to the signal to cancel the peak, the in-band distortion and OoB radiation are increased by

$$\begin{cases} \Delta p_{in} = \sum_{l=-L/2+1}^{L/2} |G'[l]|^2, \\ \Delta p_o = \sum_{l=L/2+2}^{3L/2+1} |G'[l]|^2 + \sum_{l=-3L/2}^{-(L+2)/2} |G'[l]|^2. \end{cases} \quad (15)$$

Let the total transmission power S_t be constant, i.e., $S_t = \sum_{m=1}^M S^{(m)}$, where $S^{(m)}$ is the average signal power at the m -th transmit antenna. Let $|A_p^{(m,i)}|$ denote the difference between the threshold value and the i -th peak amplitude $x_{max}^{(i)}$ at the m -th antenna. EVM increase is expressed as $\frac{1}{S_t} |A_p^{(m,i)}|^2 \Delta p_{in}$ when the PC signal is added to suppress the i -th peak amplitude $x_{max}^{(i)}$.

We calculate an average EVM value overall antennas as

$$\Delta \varepsilon_e^{(i)} = \sum_{m=1}^M \frac{1}{S_t} |A_p^{(m,i)}|^2 \Delta p_{in} = \frac{\Delta p_{in}}{S_t} \sum_{m=1}^M |A_p^{(m,i)}|^2, \quad (16)$$

where Δp_{in} denotes the pre-determined constant. The averaged EVM value $\varepsilon_e^{(i)}$ is recursively calculated as

$$\varepsilon_e^{(i)} = \varepsilon_e^{(i-1)} + \Delta \varepsilon_e^{(i-1)}. \quad (17)$$

In order to restrict OoB radiation below the permissible value, we propose to estimate the instantaneous ACLR at each antenna as follows: When the i -th PC signal is added, the ACLR at each antenna is increased as

$$\Delta \varepsilon_a^{(m,i)} = \frac{1}{S_t/M} |A_p^{(m,i)}|^2 \Delta p_o = \frac{M \Delta p_o}{S_t} |A_p^{(m,i)}|^2. \quad (18)$$

Using the above relation, the ACLR $\varepsilon_a^{(m,i)}$ after adding the i -th PC signal is recursively calculated as

$$\varepsilon_a^{(m,i)} = \varepsilon_a^{(m,i-1)} + \Delta \varepsilon_a^{(m,i)}. \quad (19)$$

Finally, the maximum value is calculated as

$$\varepsilon_a^{(i)}_{max} = f(\varepsilon_a^{(m,i)})_{max:m}, \quad (20)$$

where $f(\cdot)_{max:m}$ is a function that selects the maximum value from possible ones with respect to antenna index m . From the practical design point of view Eq. (16) maybe used to directly calculate the level of degradation per subcarrier by simply reading out the signal amplitude level $A_p^{(m,i)}$ at the transmitter end.

The PC signal scaling and peak cancellation procedure in next step is done if both the average EVM $\varepsilon_e^{(i)}$ in Eq. (17) and the maximum ACLR $\varepsilon_a^{(i)}_{max}$ in Eq. (20) are less than the pre-defined levels.

(Step 5) PC Signal Scaling and Peak Cancellation

To carry out the peak cancellation (i.e., the PC signal addition), both the averaged EVM values $\varepsilon_e^{(i)}$ and the estimated maximum ACLR $\varepsilon_a^{(i)}_{max}$ must be less than permissible values. Our proposed scheme can satisfy this condition automatically as explained below. First, when the maximum amplitude of the signal $x(t_0)$ exceeds the threshold value, the scaled PC signal is expressed as

$$\begin{aligned} p_r(t - t_0) &= -A_p \frac{1}{L} w(t - t_0) \sum_{l=-L/2+1}^{L/2} p(t - t_0) e^{j(\omega_l(t-t_0)+\theta_0)} \\ &\equiv -A_p e^{j\theta_0} g'(t - t_0), \end{aligned} \quad (21)$$

where $A_p = |x(t_0)| - A_{th}$. θ_0 is the phase of the signal $x(t_0)$. Assume that the maximum amplitude exceeds the peak detection threshold at time instance $t_0^{(i)}$. Then, the amplitude of the OFDM signal after canceling the i -th peak amplitude is represented as

$$x^{(i)}(t) = x^{(i-1)}(t) + p_r^{(i)}(t - t_0^{(i)}). \quad (22)$$

The above procedures are continued repeatedly until all amplitudes are suppressed below the peak detection threshold or the number of PC signal additions reaches a maximum number. However, if either the estimated ACLR or EVM exceeds the permissible value, the peak cancellation procedure stops before it reaches the maximum number. This stopping criterion guarantees that ACLR and EVM never exceed their permissible values.

V. BER ANALYSIS OF OFDM WITH THE DESIGNED PEAK CANCELLATION

In this section, we analyze theoretical BERs of single antenna OFDM and linear precoded (E-SDM) MIMO-OFDM with our designed peak cancellation, respectively.

A. Single antenna OFDM

In this section, first, we consider QPSK-OFDM signal whose subcarrier's I and Q-phases take either A or $-A$. Let x_e denote a random variable which expresses signal distortion due to peak cancellation. Thus, the signal after peak cancellation is given as $\pm A + x_e$. We assume that x_e follows Gaussian distribution with variance σ_e^2 and average value \bar{x}_e ;

$$p_e(x_e) = \frac{1}{\sqrt{2\pi}\sigma_e} \exp\left(-\frac{(x_e - \bar{x}_e)^2}{2\sigma_e^2}\right), \quad (23)$$

where σ_e^2 and \bar{x}_e are variance and average amplitude of x_e . Since the average power of the signal is decreased after peak cancellation, it can be intuitively seen that \bar{x}_e decreases as A_{th} decreases, while σ_e increase as A_{th} decreases. Hence, the average value of x_e can be expressed with S_{in} as

$$\bar{x}_e \approx -\alpha\sqrt{S_{in}/L}, \quad (24)$$

where L denotes the number of subcarriers. α is a constant depending on PC signal waveform $g'(t)$ given as

$$\alpha = \frac{\int_{-\infty}^{\infty} f_c(\text{Re}[g'(t)])dt}{\int_{-\infty}^{\infty} |\text{Re}[g'(t)]|dt}. \quad (25)$$

where $f_c(x)$ denotes a clipping function defined as

$$f_c(x) = \begin{cases} x & x > 0 \\ 0 & \text{otherwise.} \end{cases} \quad (26)$$

The numerator and the denominator in Eq.(25) show integral of positive side PC signal amplitude and that of its absolute value, respectively. The variance of x_e is given as

$$\sigma_e^2 = \langle (A + x_e - \mu A)^2 \rangle = \mu^2(S_{in}/L),$$

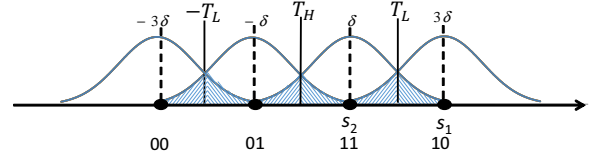
where $\mu = 1 - \bar{x}_e/A$. Here, $\langle x \rangle$ denotes expected value of the variable x .

Let x_n denote additive white Gaussian noise (AWGN) with average level A and variance σ_n^2 , i.e., PDF of x_n is given as

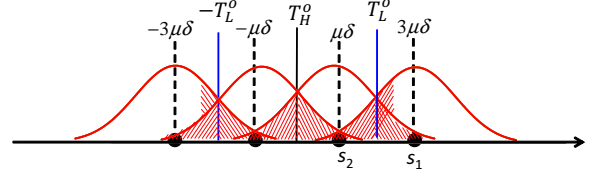
$$p_n(x_n, \sigma_n) = \frac{1}{\sqrt{2\pi}\sigma_n} \exp\left(-\frac{x_n^2}{2\sigma_n^2}\right). \quad (27)$$

x_e and x_n are Independent and identically distributed (i.i.d.) random variables and therefore PDF of mixed variable $x = x_e + x_n$ is given as convolution of $p_x(x)$ and $p_n(x)$:

$$\begin{aligned} p(x, \sigma_n, \sigma_e, \beta) &= \int_{-\infty}^{\infty} p_e(x - y, \sigma_e, \beta) p_n(y, \sigma_n) dy \\ &= \frac{1}{\sqrt{2\pi((\sigma_e^2/\beta) + \sigma_n^2)}} \exp\left(-\frac{(x - (\bar{x}_e/\sqrt{\beta}))^2}{2((\sigma_e^2/\beta) + \sigma_n^2)}\right), \end{aligned}$$



(a) w/o peak cancellation (in the presence of AWGN).



(b) w/ peak cancellation (in the presence of AWGN and signal distribution).

Fig. 6. 16QAM signal distribution (I-phase or Q-phase).

where β denotes channel gain. BER for QPSK-OFDM signal after peak cancellation in AWGN condition with channel gain is expressed as

$$\begin{aligned} P_b(A, \sigma_n, \sigma_e, \beta) &= \int_{-\infty}^0 p(x - A, \sigma_n, \sigma_e, \beta) dx \\ &= \int_0^{\infty} \frac{1}{\sqrt{2\pi((\sigma_e^2/\beta) + \sigma_n^2)}} \exp\left(-\frac{(x - (\bar{x}_e/\sqrt{\beta}))^2}{2((\sigma_e^2/\beta) + \sigma_n^2)}\right) dx, \end{aligned} \quad (28)$$

where A denotes I and Q phase signal amplitudes.

The above discussion can be extended to multi-level QAM such as 16QAM and 64QAM. The same manner as QPSK case can be used for deriving BER expressions in QAM case except that variance of in-band noise is different, e.g., for 16QAM and 64QAM cases, their variances σ_e^{16QAM} and σ_e^{64QAM} are respectively given as

$$\sigma_e^{16QAM} = \sigma_e/2, \quad (29)$$

$$\sigma_e^{64QAM} = \sigma_e/4, \quad (30)$$

where σ_e denotes variance in QPSK case. More generally, variance for 2^Q QAM is given as σ_e/Q

Figure 6 shows I-phase or Q-phase signal distribution of 16QAM at a certain subcarrier in the case with and without peak cancellation. Error probability of higher order bit P_{eH} is given as a probability that signal S_1 and S_2 exceed threshold T_H ;

$$\begin{aligned} P_{eH} &= \frac{1}{2} \frac{1}{\sqrt{2\pi}\sigma_n} \left\{ \int_0^{\infty} \exp\left(-\frac{(x + \delta)^2}{2\sigma_n^2}\right) dx \right. \\ &\quad \left. + \int_0^{\infty} \exp\left(-\frac{(x + 3\delta)^2}{2\sigma_n^2}\right) dx \right\}. \end{aligned} \quad (31)$$

Error probability of lower order bit of 16QAM is given as a

probability that signal S_1 and S_2 exceed threshold T_L ;

$$P_{eL} = \frac{1}{2} \frac{1}{\sqrt{2\pi}\sigma_n} \left\{ \int_{-2\delta}^{2\delta} \exp\left(-\frac{(x+3\delta)^2}{2\sigma_n^2}\right) dx + \int_{-\infty}^{-2\delta} \exp\left(-\frac{(x+\delta)^2}{2\sigma_n^2}\right) dx + \int_{2\delta}^{\infty} \exp\left(-\frac{(x+\delta)^2}{2\sigma_n^2}\right) dx \right\}. \quad (32)$$

On the other hand, as illustrated in Fig.6(b), the average power of the signal and its distribution are reduced by peak cancellation.

Since it is clear that the optimum decision threshold for higher order bit is $T_H^o = 0$, error probability of higher order bit is given as

$$\hat{P}_{eH}(T_H^o = 0) = \frac{1}{2} \frac{1}{\sqrt{2\pi}(\sigma_n^2 + (\sigma_e^2/\beta))} \cdot \left\{ \int_{T_H^o=0}^{\infty} \exp\left(-\frac{(x+\mu\delta/\sqrt{\beta})^2}{2(\sigma_n^2 + (\sigma_e^2/\beta))}\right) dx + \int_{T_H^o=0}^{\infty} \exp\left(-\frac{(x+3\mu\delta/\sqrt{\beta})^2}{2(\sigma_n^2 + (\sigma_e^2/\beta))}\right) dx \right\}. \quad (33)$$

Error probability of lower order bit of Gray-coded 16QAM using the optimum decision threshold T_L^o in AWGN condition in the case with peak cancellation is

$$\hat{P}_{eL}(T_L^o) = \frac{1}{2} \frac{1}{\sqrt{2\pi}(\sigma_n^2 + (\sigma_e^2/\beta))} \cdot \left\{ \int_{-T_L^o}^{T_L^o} \exp\left(-\frac{(x+3\mu\delta/\sqrt{\beta})^2}{2(\sigma_n^2 + (\sigma_e^2/\beta))}\right) dx + \int_{-\infty}^{-T_L^o} \exp\left(-\frac{(x+\mu\delta/\sqrt{\beta})^2}{2(\sigma_n^2 + (\sigma_e^2/\beta))}\right) dx + \int_{T_L^o}^{\infty} \exp\left(-\frac{(x+\mu\delta/\sqrt{\beta})^2}{2(\sigma_n^2 + (\sigma_e^2/\beta))}\right) dx \right\}. \quad (34)$$

The optimum decision threshold $T_L^o = -2\mu\delta/\sqrt{\beta}$ to minimize BER can be derived by $\frac{\partial P_{eL}(T_L^o)}{\partial T_L^o} = 0$. Details of the derivation are given in the Appendix. Average BER is given by averaging Eq.(33) and Eq.(34).

B. E-SDM MIMO-OFDM

In this subsection, we consider an Eigen-beam space division multiplexing (E-SDM) OFDM in $M \times N$ MIMO systems, where M and N denotes number of transmit antenna and the number of receive antennas, respectively. Hereafter, we assume $M = 4$ and $N = 2$ as an example. PDFs of eigen values with order for random $M \times N$ MIMO channel matrix are given as [11]:

$$f_1(\lambda_1) = \Phi_1(\lambda_1) \exp(-\lambda_1) + \Phi_2(\lambda_1) \exp(-2\lambda_1), \quad (35)$$

$$f_2(\lambda_2) = -\Phi_1(\lambda_2) \exp(-2\lambda_2), \quad (36)$$

where

$$\Phi_1(\lambda) = \lambda^2 \left(\frac{1}{6} \lambda^2 - \lambda + 2 \right),$$

$$\Phi_2(\lambda) = \lambda^2 \left(\frac{1}{6} \lambda^2 + \lambda + 2 \right).$$

Thus, BER expression of signal transmission over the i -th eigen channels in $M \times N$ MIMO channel can be derived as

$$P_b^{(i)} = \int_0^{\infty} f_i(\lambda) \left(\int_0^{\infty} p(\lambda, x) dx \right) d\lambda, \quad (37)$$

where M and N denote the number of transmit and receive antennas. $p(\lambda, x)$ denotes PDF of the signal after peak cancellation in presence of AWGN and λ_i is the i -th eigen vector. Similarly single antenna case, for QPSK transmission over i -th eigen channel,

$$p(\lambda, x) = \frac{1}{\sqrt{2\pi}(\sigma_n^2/\lambda + \sigma_e^2 A^2 \lambda)} \exp\left(-\frac{(x - \bar{x}_e A \sqrt{\lambda} - A)^2}{2(\sigma_e^2 A^2 \lambda + \sigma_n^2/\lambda)}\right).$$

Average BER over the first and second eigen channel is given as

$$\bar{P}_b = \frac{P_b^{(1)} + P_b^{(2)}}{2}, \quad (38)$$

where the same power is allocated to the first and the second eigen channels.

VI. PERFORMANCE RESULTS AND DISCUSSIONS

To clarify the validity of the proposed framework, we evaluate the performance of MIMO-OFDM system by computer simulation. The system block diagram is shown in the same as in Fig. 1. We assume QPSK, 16QAM, or 64QAM data modulation. The number of FFT points is 512 and the number of subcarriers is 64. In MIMO cases, Eigen-mode precoding is adopted at each sub-carrier (i.e., E-SDM MIMO), where the transmitter and the receiver equip N and M antennas, respectively. The number of streams is denoted as K . Here, we assume $K = N$. Channel model is independent attenuated 6-path Rayleigh fading. The requirement of ACLR is set to -50 dB, while those of EVM are set to -20 , -25 , and -30 dB for QPSK, 16QAM, and 64QAM cases, respectively. In this paper, we assume that channel estimation is perfectly done at the receiver and channel state information is ideally shared with the transmitter.

One of the conventional approaches is repeated C&F [18]-[19]. The block diagram is shown in Fig. 7, where $x(t)$ and $x_o(t)$ are the OFDM signals before clipping and after filtering. To reduce the computational complexity, only the clipped signal (i. e., the peak amplitude exceeds a peak detection threshold) is band-limited by filtering operation. Unlike the proposed peak cancellation, this method needs to empirically optimize the filter parameters so as to keep EVM and ACLR values below these pre-defined thresholds.

We also evaluate prior limiter based techniques in [31]-[32]. In [31], the peak detection threshold at n -th iteration $A_{th}^{(n)}$ in repeated C&F is adaptively determined as

$$A_{th}^{(n)} = \sqrt{\frac{N_f}{N_p}} A_{th}^{(n-1)}, A_{th}^{(0)} = \frac{1}{N_f} \sum_{s=0}^{N_f-1} |x(s\Delta t)|, \quad (39)$$

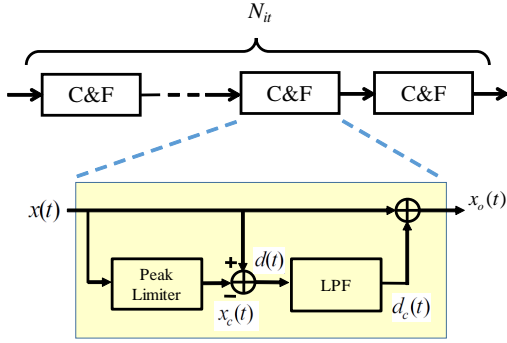


Fig. 7. Block diagram of repeated C&F, where N_{it} denotes the number of iterations.

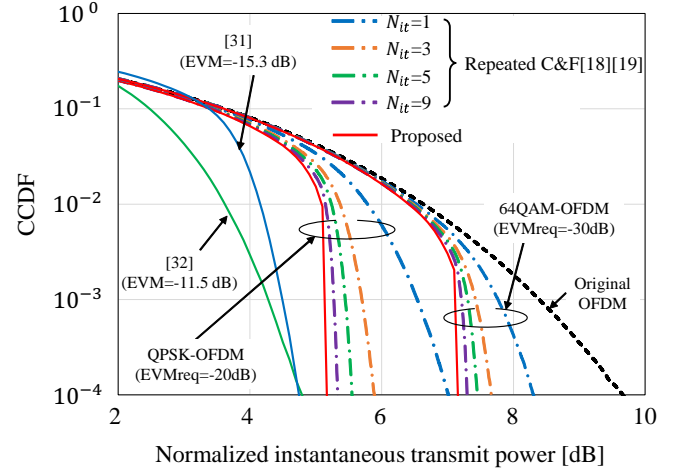
where $x(s\Delta t)$ denotes the transmit signal before C&F operation and Δt denotes sampling interval. N_f and N_p are the number of FFT points and the number of OFDM samples exceeding $A_{th}^{(n-1)}$, respectively. In [32], the following nonlinear function is used to limit peak amplitude:

$$y(s\Delta t) = A_{th} \frac{x(s\Delta t)}{|x(s\Delta t)|} \left(1 + \left(\frac{v}{|x(s\Delta t)|} \right)^{(1/a)} \right)^{-a}, \quad (40)$$

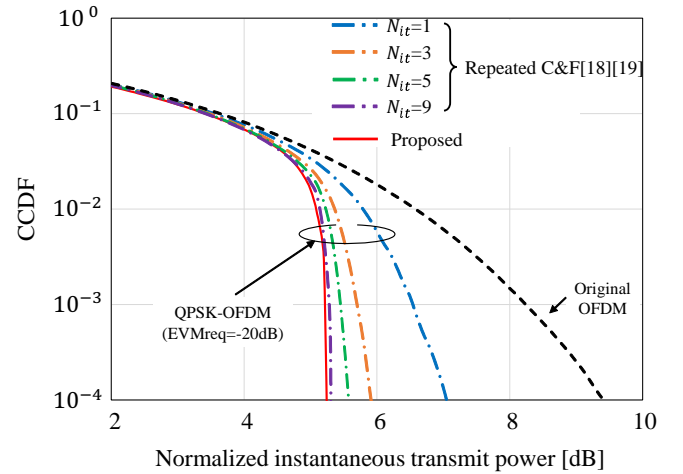
where $x(s\Delta t)$ and $y(s\Delta t)$ are input and output complex time-domain signals of the companding function, respectively. $|x(s\Delta t)|$ denotes the absolute value of $x(s\Delta t)$. A_{th} is the maximum amplitude of $|y(s\Delta t)|$. v and a are non-linear parameters of the nonlinear function, respectively.

A. PAPR

Figures 8(a) and (b) illustrate the statistical distribution of the normalized instantaneous signal power of transmitting signals in single-antenna OFDM and 4×2 MIMO-OFDM, respectively. Here, we use CCDF to evaluate the statistical distribution and the instantaneous is normalized by average power of the signal. For comparison, CCDFs of cases of repeated C&F in [18][19] and other limiter based approaches in [31][32] are also shown. In repeated C&F [18][19], we note here that both ACLR and EVM satisfy the required values. In [32], $v=7$, $a = 0.05$ and $A_{th} = 1$ are used. In [31][32], roll-off filter with roll-off factor = 0 is used. Figure 8(a) shows that the instantaneous power of transmit signal with the proposed method is limited to around 5.12 dB and 7.25 dB at $\text{CCDF}=10^{-4}$ for QPSK and 64QAM data modulation schemes. The optimum threshold value is $P_{th}=5.12$ dB and 7.25 dB for QPSK and 64QAM data modulation schemes, respectively. Note that the achieved PAPR by the proposed method is close to the optimum threshold value. In other words, the threshold value corresponds to the achievable PAPR. As for comparison with other approaches, although methods in [31][32] show lower PAPR than the proposed method, it suffers from high in-band distortion which results in BER degradation as discussed in Fig. 12(b). Note that the proposed method is able to reduce the PAPR to a lower value compared to [31][32] if the required EVM value is



(a) $M=N=1$.



(b) $M=4, N=2, K=2$.

Fig. 8. CCDF of normalized instantaneous transmit power, where N_{it} denotes the number of iterations in repeated C&F.

set to a higher value, because the proposed method works to automatically minimize the peak power under given EVM and ACLR requirements. It can be also seen that instantaneous power in the case of repeated C&F is approaching the proposed method by increasing the number of iterations in the repeated C&F; almost the same CCDF in comparison with the proposed method is achieved with $N_{it} = 9$. Similar findings are observed in Fig. 8(b) for E-SDM case.

B. BER

Figures 9(a) and (b) illustrate the BER performance of single-antenna OFDM with the peak cancellation in AWGN channel. In this figure, peak cancellation is conducted under ACLR and EVM restrictions. Here, QPSK and 16QAM are used as subcarrier modulation. The BER curve of OFDM without any degradation due to peak cancellation is labeled as "ideal case". It is demonstrated in Fig. 9(a) that the proposed method achieves very close BER performance to ideal case, where EVM satisfies the pre-defined requirements -20 dB for QPSK and -25 dB for 16QAM, respectively. These figures

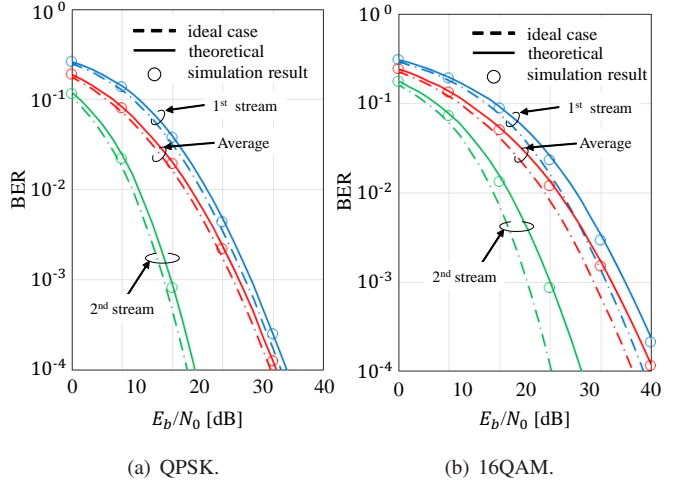
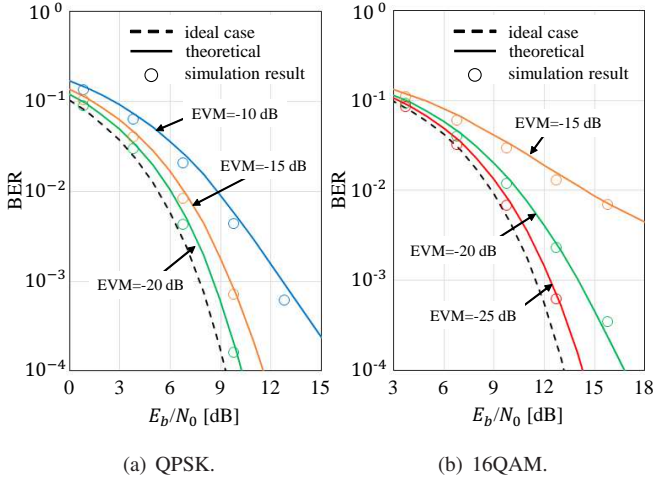


Fig. 9. Theoretical BER performance and its simulation results of OFDM system using the proposed method in AWGN channel.

Fig. 11. Theoretical BER and its simulation results of E-SDM OFDM system using the proposed method ($N=4$, $M=2$, $K=2$).

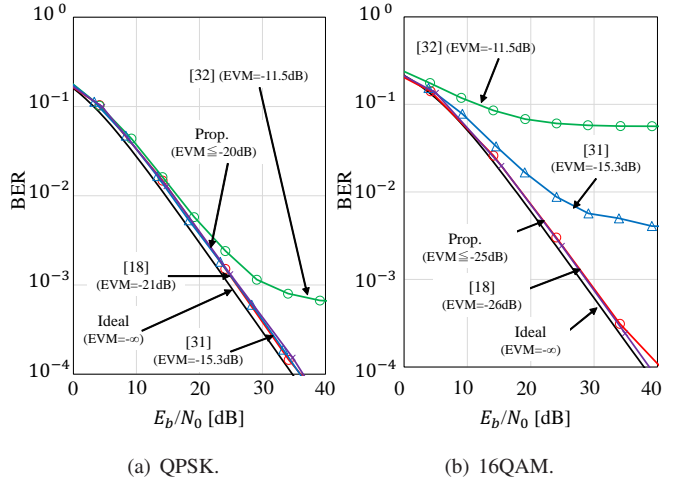
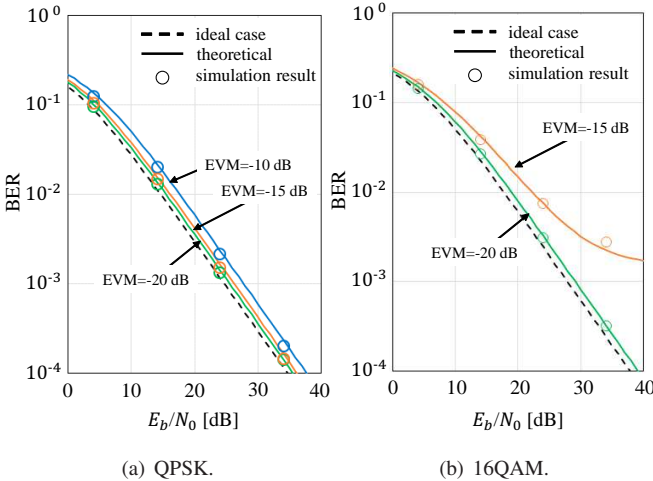


Fig. 10. Theoretical BER performance and its simulation results of OFDM system using the proposed method in Rayleigh fading channel.

Fig. 12. BER comparison of the proposed method with conventional approaches in Rayleigh fading channel, where QPSK and 16QAM are used as subcarrier modulation, respectively.

also indicate that the theoretical BER curves show good agreements with its simulation results.

Figure 10 and 11 illustrate the BER performance of single-antenna OFDM and 4×2 MIMO using eigen-mode in Rayleigh fading channel, respectively. Here QPSK and 16QAM are used as subcarrier modulation. EVM and ACLR are restricted below the pre-defined values, respectively. These figures also indicate that the theoretical BER curves show good agreements with their simulation results. It can also be seen from Fig. 11 that BER performance of the first and second streams in E-SDM scenarios show good agreements with their simulation results. We note here that EVM and ACLR meet the pre-defined values.

BER of the proposed method is compared with those of the conventional approaches in [18], [31] and [32] in Fig. 12, where QPSK and 16QAM are used for subcarrier modulation in Figs. 12(a) and Fig. 12(b), respectively. The Purple line shows the BER of the repeated C&F [18] using the same threshold as the proposed peak cancellation. The blue line and the green line show the BER of the repeated C&F in [31] and

that of the companding technique in [32], respectively. Here, parameters in the repeated C&F and companding are same in Fig. 8(a). The red line shows the BER of the proposed method. In Fig. 12, for QPSK case, it can be seen that the proposed method and conventional methods in [18][31] show almost the same BER. On the other hand, for 16QAM case, BER of the conventional methods are significantly degraded, while the proposed method shows good BER performance comparable to the ideal case. This is because the proposed method is able to keep EVM below the predefined threshold automatically unlike the conventional methods.

C. Complexity

This subsection evaluates a computational complexity of required PAPR reduction procedures between the two methods above. In this comparison, the number of complex multiplications is used as the complexity metric. When PC signal is added N_{pc} times per OFDM symbol, the complexity of

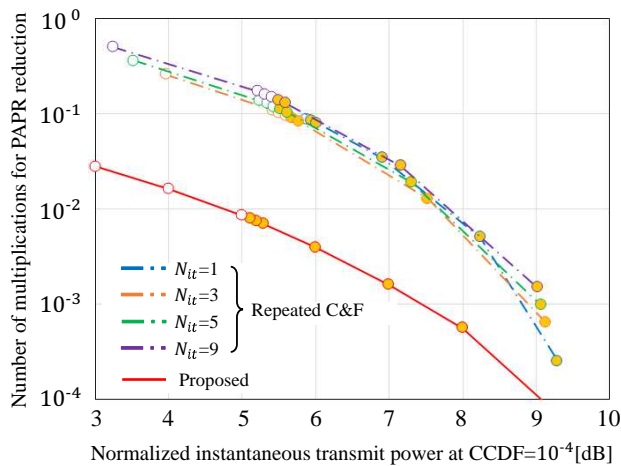


Fig. 13. Number of multiplications per OFDM symbol for PAPR reduction ($M = 4$, $N = 2$, $K = 2$), where QPSK is adopted as subcarrier modulation.

the proposed method is $\langle N_w \times N_{pc} \rangle$, where N_w denotes the number of complex multiplications per PC addition. On the other hand, the complexity of the C&F with time domain LPF is given as $\langle \sum_{j=1}^{N_{it}} (N_{tap} \times N_{th}^{(j)}) \rangle$. Here, $\langle x \rangle$ denotes the averaging of x . N_{it} and N_{tap} denote the number of iterations and the number of taps in time domain filter, respectively. $N_{th}^{(j)}$ is the number of samples exceeding a given threshold per OFDM symbol. j denotes the iteration index.

The required complexity for the peak cancellation in SDM-OFDM is evaluated in comparison with the repeated C&F based on the above defined metric in Fig. 13 where $M = 4$ and $N = 2$ are assumed. In the figure, we assume QPSK is adopted as subcarrier modulation. Here, PAPR is defined as the normalized instantaneous power observed at $CCDF=10^{-4}$. The red line shows the result of the proposed method, while the results of repeated C&F method are depicted by other color lines. The color-fill circular shape markers represent that both EVM and ACLR requirements are fulfilled, while the white-fill shows that either EVM or ACLR (or both) exceed the pre-defined value. In repeated C&F cases, normalized instantaneous power is approaching the peak detection threshold $S_{th} = 10 \log_{10} \frac{A_{th}^2}{S_t}$ by repeating clipping and filtering operations. Note that in the proposed method, ACLR and EVM can be kept below the required values automatically, unlike the repeated C&F method. This figure proves that the required complexity for the proposed peak cancellation is lower in comparison with the repeated C&F.

D. Windowing

Figure 14 illustrates the relationship between the required complexity and achievable ACLR as a function of window size truncating the PC signal in terms of required EVM values which are set to -20 , -25 or -30 dB, where red drawn circle markers denote selected window size for each EVM value in case of $ACLR = -50$ dB. The threshold is selected to meet the required EVM as discussed in Sect. IV and correspond to achievable PAPR and BER. The PC signal is truncated by

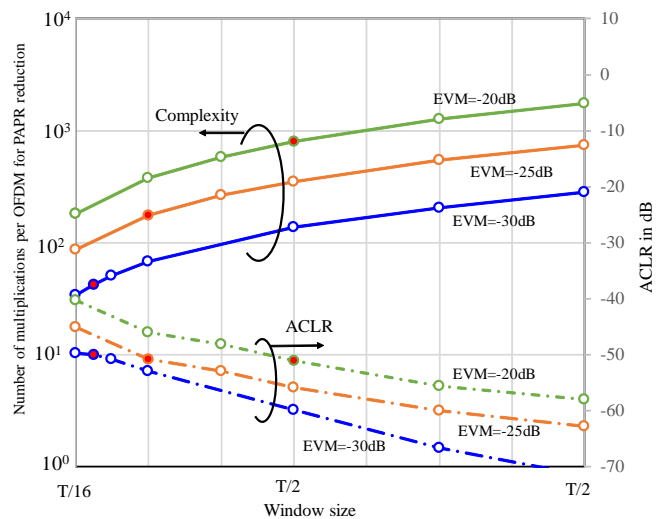


Fig. 14. Relationship between complexity and ACLR in terms of required EVM, where peak detection threshold values are set to optimum values to meet EVM requirements.

the window function $w(t)$ as shown by Eqs. (6)-(8). Thus, window-size T_2 affects both ACLR and the complexity. It can be seen that from this figure as window-size increases, ACLR decreases at the expense of increasing the required complexity. The results suggest that the required complexity is minimized by optimizing the window-size under a given EVM (i.e., BER) and threshold value (i.e., PAPR).

VII. CONCLUSION

Performance analysis of a dynamic peak-cancellation scheme for E-SDM OFDM system has been presented, where EVM and ACLR are automatically restricted below a pre-defined level. Using the proposed approach, degradations due to ACLR and EVM are effectively mitigated while keeping the OoB radiation below its target value. Furthermore, practical design of peak-cancellation signal is discussed with target OoB radiation and in-band distortion through optimizing the windowing size of the PC signal. In addition, we have also theoretically analyzed peak cancellation capability and achieved BER, respectively. Numerical results prove that our peak cancellation method is effective in improving both the BER and PAPR under EVM and ACLR restrictions. It can be also seen that theoretical BER show good agreements with simulation results.

APPENDIX

The derivation of T_L^o in Eq. (34) is as follows. Without loss of generality, we assume $\beta=1$. Since Gray-encoded 16QAM is used, the error probability of lower- order bits is given as

$$\begin{aligned} \hat{P}_{eL}(T_L) &= \frac{1}{2} \frac{1}{\sqrt{2\pi(\sigma_n^2 + \sigma_e^2)}} \cdot \\ &\quad \left\{ \int_{-T_L}^{T_L} \exp\left(-\frac{(x+3\mu\delta)^2}{2(\sigma_n^2 + \sigma_e^2)}\right) dx \right. \\ &\quad + \int_{-\infty}^{-T_L} \exp\left(-\frac{(x+\mu\delta)^2}{2(\sigma_n^2 + \sigma_e^2)}\right) dx \\ &\quad \left. + \int_{T_L}^{\infty} \exp\left(-\frac{(x+\mu\delta)^2}{2(\sigma_n^2 + \sigma_e^2)}\right) dx \right\} \\ &= 1 + \operatorname{erf}\left(\frac{T_L + 3\mu\delta}{\sqrt{2(\sigma_n^2 + \sigma_e^2)}}\right) \\ &\quad - \operatorname{erf}\left(\frac{T_L + \mu\delta}{\sqrt{2(\sigma_n^2 + \sigma_e^2)}}\right), \end{aligned} \quad (41)$$

where T_L is the threshold level to decide I and Q phase of 16QAM constellation points. Using the relationship

$$\int \frac{1}{\sqrt{2\pi\sigma_n^2}} \exp\left(-\frac{x^2}{2\sigma_n^2}\right) dx = \frac{1}{2} \left(1 + \operatorname{erf}\left(\frac{x}{\sqrt{2\sigma_n^2}}\right)\right), \quad (42)$$

the partial differentiation of $\hat{P}_{eL}(T_L)$ with respect to T_L is given as

$$\begin{aligned} \frac{\partial \hat{P}_{eL}(T_L)}{\partial T_L} &= \frac{1}{\sqrt{2(\sigma_n^2 + \sigma_e^2)}} \cdot \\ &\quad \left(\exp\left(\frac{(T_L + 3\mu\delta)^2}{2(\sigma_n^2 + \sigma_e^2)}\right) \right. \\ &\quad \left. - \exp\left(\frac{(T_L + \mu\delta)^2}{2(\sigma_n^2 + \sigma_e^2)}\right) \right). \end{aligned} \quad (43)$$

By solving $\frac{\partial \hat{P}_{eL}(T_L^o)}{\partial T_L^o} = 0$,

$$\begin{aligned} \exp\left(\frac{(T_L^o + 3\mu\delta)^2}{2(\sigma_n^2 + \sigma_e^2)}\right) &= \exp\left(\frac{(T_L^o + \mu\delta)^2}{2(\sigma_n^2 + \sigma_e^2)}\right) \\ (T_L^o + 3\mu\delta)^2 &= (T_L^o + \mu\delta)^2 \\ T_L^o &= -2\mu\delta, \end{aligned} \quad (44)$$

where $-2\mu\delta$ is an intersection point of two Gaussian distributions located on the left side of the horizontal axis of 16QAM constellation as shown in Fig. 6(b).

ACKNOWLEDGMENT

This research was supported in part by JSPS KAKENHI (JP17K06427, JP17J04710), and Kyushu University Short-term International Research Exchange Program by University Research Administration Office.

REFERENCES

- [1] T. Hwang, C. Yang, G. Wu, S. Li, and G. Ye Li, "OFDM and Its Wireless Applications: A Survey," *IEEE Trans. Vehic. Tech.*, Vol.58, No.4, pp.1673-1694, May 2009.
- [2] Y. Akaiwa, "Introduction to Digital Mobile Communication, 2nd Edition," Wiley, June 2015.
- [3] S.H.Han and J.H.Lee, "An Overview of Peak-to-Average Power Ratio Reduction Techniques for Multicarrier Transmission," *IEEE Wireless Communications*, pp.57-65, April 2005.
- [4] Y. Rahmatallah and S. Mohan, "Peak-To-Average Power Ratio Reduction in OFDM Systems: A Survey And Taxonomy," *IEEE Commun. Surveys & Tutorials*, vol.15, no.4, pp.1567-1592, 2013.
- [5] R. W. Bauml, R.F. H. Fischer and J. B. Huber, "Reducing the peak-to-average power ratio of multicarrier modulation by selected mapping," *Electron. Lett.*, vol.32, no.22, pp.2056-2057, Oct. 1996.
- [6] D.-W. Lim, J.-S. No, C.-W. Lim, and H. Chung, "A New SLM OFDM Scheme With Low Complexity for PAPR Reduction," *IEEE Signal Processing Letters*, Vol. 12, No. 2, Feb. 2005.
- [7] S. H. Müller and J. B. Huber, "OFDM with reduced peak-to-average power ratio by optimum combination of partial transmit sequence," *Electron. Lett.*, vol.33, no.5, pp.368-369, Feb. 1997.
- [8] L. J. Cimini and N. R. Sollenberger, "Peak-to-Average Power ratio reduction of an OFDM signal using partial transmit sequence," *IEEE Commun. Lett.*, vol.4, no.3, pp.86-88, March 2000.
- [9] O. Muta and Y. Akaiwa, "Weighting Factor Estimation Method for Peak Power Reduction Based on Adaptive Flipping of Parity Bits in Turbo-Coded OFDM Systems," *IEEE Trans. Vehicular Technology*, vol.57, no.6, Nov. 2008.
- [10] O. Muta, "Construction and Blind Estimation of Phase Sequences for Subcarrier-phase Control Based PAPR Reduction in LDPC-Coded OFDM Systems," *IEICE Trans. Fundamentals*, vol.E93-A, no.11, Nov. 2010.
- [11] J. Tellado and J. M. Cioffi, "Efficient algorithms for reducing PAPR in multicarrier systems," *IEEE International Symposium on Information Theory*, p. 191, Aug. 1998.
- [12] P. Boonsrimuang, K. Mori, T. Paungma, and H. Kobayashi, "Proposal of Simple PAPR Reduction Method for OFDM Signal by Using Dummy Sub-Carriers," *IEICE Trans. Commun.*, vol.E91.B, no.3, pp.784-794, March 2010.
- [13] B. S. Krongold and D. L. Jones, "PAR Reduction in OFDM via Active Constellation Extension," *IEEE Trans. Broadcast.*, vol. 49, no. 3, pp. 258-268, Sept. 2003.
- [14] T. A. Wilkinson, and A. E. Jones, "Minimization of the peak to mean envelope power ratio of multicarrier transmission schemes by block coding," in *Proc. IEEE Vehicular technology Conf.*, pp.825-829, 1995.
- [15] A. E. Jones and T. A. Wilkinson, "Combined coding for error control and increased robustness to system nonlinearities in OFDM," in *Proc. IEEE Vehicular technology Conf.*, pp.904-908, 1996.
- [16] S. Shepherd, J. Orriss, and S. Barton, "Asymptotic limits in peak envelope power reduction by redundant coding in orthogonal frequency-division multiplex modulation," *IEEE Trans. Commun.*, vol.45, no.1, pp.5-10, Jan. 1998.
- [17] X. Li and L. J. Cimini, "Effect of clipping and filtering on the performance of OFDM," *IEEE Commun. Lett.*, vol.2, no.5, pp.131-133, May 1998.
- [18] J. Armstrong, "Peak-to-average power reduction for OFDM by repeated clipping and frequency domain filtering," *Electron. Letters*, vol.38, no.5, pp.246-247, Feb. 2002.
- [19] S. Tomisato and H. Suzuki, "A peak reduction scheme based on control signal insertion for multi-carrier mobile communication," *IEICE Trans. Commun.*, vol. E86-B, no.6, pp. 1910-1916, June 2003.
- [20] M. M. Lee and Y. Kim, "An adaptive clipping and filtering technique for PAPR reduction in OFDM systems," *Circuits Syst. Signal Process.* Vol.32, no.3, pp.1335-1349, Jun. 2013.
- [21] M. Pauli and H.-P. Kuchenbecker, "Minimization of the Intermodulation Distortion of a Nonlinearly Amplified OFDM Signal," *Wireless Personal Commun.*, Vol.4 pp.93-101, 1996.
- [22] X. Huang, J. Lu, J. Zheng, K. B. Letaief, and J. Gu, "Companding transform for reduction in peak-to-average power ratio of OFDM signals," *IEEE Trans. Wireless Commun.*, vol. 3, Issue 6, pp. 2030-2039, Nov. 2004.
- [23] T. Jiang, Y. Yang, and Y. Song, "Exponential companding technique for PAPR reduction in OFDM systems," *IEEE Trans. Broadcasting*, vol.51, no.2, pp.244-248, June 2005.
- [24] L. Dan, T. Li, Y. Xiao, and S. Li, "Performance of peak cancellation for PAPR reduction in OFDM system," *International Conference on Communications, Circuits and Systems*, 2008.

- [25] Y. Huang, "A Simplified Peak Cancellation Method for OFDM Signals," International Conference on Computer Science and Electronics Engineering ICCSEE, 2012.
- [26] T. Hino, O. Muta, and H. Furukawa, "A Study on Peak Amplitude Suppression of OFDM Signals under Restriction of Out-of-Band Radiation Power," The Transactions of IEICE B, Vol.J97-B, No.6, Jun. 2014 (in Japanese).
- [27] T. Kageyama, O. Muta, and H. Gacanin "An Adaptive Peak Cancellation Method for Linear-Precoded MIMO-OFDM Signals," Proc. PIMRC'15, Sept. 2015.
- [28] Y.-C. Wang and A.-Q. Luo, "Optimized iterative clipping and filtering for PAPR reduction of OFDM signals," IEEE Trans. Commun., vol. 59, no. 1, pp. 33-37, Jan. 2011.
- [29] X. Zhu, W. Pan, H. Li and Y. Tang, "Simplified approach to optimized iterative clipping and filter for PAPR reduction of OFDM signals," IEEE Trans. Commun., vol.61, no.5, pp.1891-1901, May. 2013.
- [30] I. Sohn and S. C. Kim, "Neural network based simplified clipping and filtering technique for PAPR reduction of OFDM signals," *IEEE Commun. Lett.*, vol.19, no.8, pp.1438-1441, Aug. 2015.
- [31] K. Anoh, C. Tanriover, B. Adebisi and M. Hammoudeh, "A new approach to iterative clipping and filtering PAPR reduction scheme for OFDM systems," IEEE Access, vol.6, pp.17533-17544, Sept. 2017.
- [32] B. Adebisi, K. Anoh and K. M. Rabie, "Enhanced nonlinear companding scheme for reducing PAPR of OFDM systems," IEEE Systems journal, vol.13, issue 1, Mar. 2019.